Inorganic Chemistry

Article

pubs.acs.org/IC

Metastable 11 K Superconductor $Na_{1-y}Fe_{2-x}As_2$

Gina M. Friederichs,[†] Inga Schellenberg,[‡] Rainer Pöttgen,[‡] Viola Duppel,[¶] Lorenz Kienle,[§] Jörn Schmedt auf der Günne,[†] and Dirk Johrendt*[,†]

[†]Department Chemie, Ludwig-Maximilians-Universtiät München, Butenandtstrasse 5-13 (D), 81377 München, Germany

[‡]Institut für Anorganische und Analytische Chemie, Universität Münster, Corrensstrasse 30, 48149 Münster, Germany

[¶]Max-Planck-Institut für Festkörperforschung, Heisenbergstrasse 1, 70569 Stuttgart, Germany

[§]Institut für Materialwissenschaft, Christian-Albrechts-Universität Kiel, Kaiserstrasse 2, 24143 Kiel, Germany

ABSTRACT: The topochemical deintercalation of Na^+ ions from solid NaFeAs at room temperature in THF with iodine yields the superconducting phase $Na_{1-y}Fe_{2-x}As_2$ ($T_c \approx 11$ K). This metastable iron arsenide decomposes at 120 °C and is not accessible by high-temperature solid-state synthesis. X-ray powder diffraction confirms the $ThCr_2Si_2$-type structure, but reveals very small coherently scattering domains with a mean composition $Na_{0.9(2)}Fe_{1.7(1)}As_2$. HRTEM investigations show crystalline as well as strongly distorted areas with planar defects. The latter are probably due to sodium loss and disorder which is also detected by ^{23}Na solid state NMR. The ^{57}Fe-Mössbauer spectrum of $Na_{1-y}Fe_{2-x}As_2$ shows one type of iron atoms in tetrahedral coordination. All results point to one crystallographic phase with very small domains due to fluctuations of the chemical composition. From electronic reasons we suggest the superconducting phase is presumably $NaFe_2As_2$ in the ordered fractions of the sample.

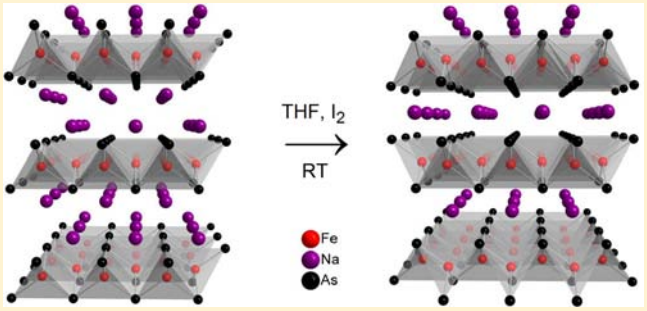

INTRODUCTION

Iron-based superconductors have inspired the field of high-temperature superconductivity research.[1] While the already achieved progress with respect to the properties and underlying physics of these materials is enormous,[2] the further development of their chemistry is still in the early stages. Currently, conventional solid-state synthesis at high temperatures yield thermodynamically stable compounds like $La(O_{1-x}F_x)FeAs$,[3] $(Ba_{1-x}K_x)Fe_2As_2$,[4] or $Na_{1-x}FeAs$,[5] and related compounds,[6] where superconductivity emerges in layers of edge-sharing $^2_\infty[(FeAs_{4/4})^-]$ tetrahedra. Several kinds of doping control the charge of these layers and move the systems from antiferromagnetic[7] to superconducting states.[8,9]

So far, the highest critical temperature (T_c) observed in iron based materials is around 55 K in $Sm(O_{0.85}F_{0.15})FeAs$,[10] thus lower than in copper-oxide superconductors. However, all known iron-based superconductors are single-layer structures, with one crystallographically independent iron atom per unit cell. Keeping in mind that often multilayer copper oxides exhibit T_c above the temperature of liquid nitrogen, higher critical temperatures might be conceivable in multilayer iron arsenides. Generally, access to artificial FeAs multilayer superstructures seems possible by pulsed laser deposition methods,[11,12] which yield thin films only. It appears at least questionable, if high temperature methods alone will be able to produce novel iron-based materials, thus access to possible multilayer superstructures may require smart methods like the soft chemistry approach.

The existence of the metastable iron arsenide $NaFe_2As_2$ with the $ThCr_2Si_2$-type (122) structure has recently been reported.[13] The authors declared a critical temperature from 12 up to 25 K, which is very high in comparison with the other known AFe_2As_2 compounds (A = K (4 K), Rb (3 K), Cs (2.6 K)). But already the existence of $NaFe_2As_2$ is remarkable, because the radius of the sodium ion was expected to be too small to fill the coordination polyhedron in the $ThCr_2Si_2$-type structure. It is thus not surprising that this compound cannot be synthesized by solid state methods at higher temperatures. Indeed, $NaFe_2As_2$ decomposes already at 120 °C.[13] A compound with the nominal composition $Na_{0.5}FeAs$ but PbFCl-type (111) structure and T_c = 12 K has also been reported.[14] Further investigations of this material are important for two reasons. First, the T_c is remarkably high within this series, but more importantly, this compound may open new pathways to iron arsenide materials by soft chemistry methods. But so far, no comprehensible and reproducible method to synthesize $NaFe_2As_2$ has been published. In the first report,[13] NaFeAs has been converted to $NaFe_2As_2$ in a not specified ionic liquid, but no further details of the experiment and the detailed composition of the product are given. According to another recent report,[15] $NaFe_2As_2$ occurred as a minor byproduct in $Na_{1-x}FeAs$ during the decomposition of NaFeAs by exposing to air or water.

Received: March 15, 2012
Published: July 18, 2012

   dx.doi.org/10.1021/ic3005618 | *Inorg. Chem.* 2012, 51, 8161−8167

In this article, we present a reproducible method to synthesize this 122-type superconductor by topochemical deintercalation of NaFeAs at room temperature. The reaction product is thoroughly characterized by X-ray powder-diffraction (PXRD), magnetic measurements, ^{57}Fe-Mössbauer spectroscopy, energy dispersive X-ray analysis (EDX), ^{23}Na solid state nuclear magnetic resonance (NMR) spectroscopy, and high resolution transmission electron microscopy (HRTEM).

RESULTS AND DISCUSSION

Synthesis. $Na_{1-y}Fe_{2-x}As_2$ was synthesized by topochemical deintercalation of sodium from solid NaFeAs with iodine as mild oxidation agent at room temperature in dried THF (Scheme 1). Mild conditions are essential due to its metastable character. The decomposition temperature was determined to be around 120 °C by DSC measurements. For the optimization of the synthesis conditions several attempts were carried out, however, neither performing the reaction at lower temperatures (−10 °C, −50 °C in THF) nor at higher temperatures (60 °C in THF, 90 °C in DMSO) yielded better sample quality. The deintercalation is a liquid−solid reaction, therefore one would expect that it starts at the surface of the particles whereby a sodium gradient arises. Presumably a sodium deficient 111-phase $Na_{1-x}FeAs$ is initially formed that becomes increasingly destabilized until it transforms to the 122-type structure. The latter requires sliding of every second FeAs-layer by 1/2 translation along the lattice parameter *b*. We assume that the structural rearrangements may not proceed homogenously in the crystals, which is probably responsible for the poor crystallinity of the samples.

Scheme 1. Synthesis of $Na_{1-y}Fe_{2-x}As_2$

$$NaFeAs \xrightarrow[THF,\ 40\ h]{0.8\ I_2} 0.5\ Na_{1-y}Fe_{2-x}As_2 + 0.5\ NaI$$

Crystal Structure. The X-ray powder diffraction (PXRD) pattern shown in Figure 1 displays a large background and broad diffraction peaks. All peak positions are consistent with a tetragonal body-centered unit cell with the lattice parameters *a* = 383.1(3) pm and *c* = 1252(2) pm, in agreement with those given for $NaFe_2As_2$ in ref.[13] Broad humps in the background near the peak positions are suggestive of certain fractions of the sample having very small coherently scattering domains. To support this assumption, we have decomposed the pattern into three components as shown in Figure 1a. First, a rather simple background function (10 parameters) describes the contributions of the capillary and the sample absorption. The second component is the scattering of very small $Na_{1-y}Fe_{2-x}As_2$ domains (~1 nm) which produces the humps. Finally we add the scattering of larger, but still small domains (~11 nm) of $Na_{1-y}Fe_{2-x}As_2$ that give rise to the peaks. The sum of these three components is already a reasonable fit of the observed pattern in Figure 1a. However, this model is still too simple to fit the pattern quantitatively. A significantly better fit results by the standard procedure with one crystalline phase and 36 background parameters (Figure 1b), which has finally been used to obtain the structure parameters compiled in Table 1. Refinements of the occupation parameters revealed the composition $Na_{0.99(4)}Fe_{1.62(2)}As_2$. Due to the small scattering power, the sodium content is relatively inaccurate. We also suggest that the Rietveld refinement slightly overestimates the sodium occupation, because only domain sizes larger than ~11 nm are considered, while the scattering of smaller domains with probably less sodium is covered by the background function. Nevertheless, our analysis shows that the sample is one crystallographic phase, and the background as well as the broad peaks can be explained by small domain sizes and fluctuations of the chemical composition. The latter is confirmed by the EDX nanoprobe analysis of several areas.

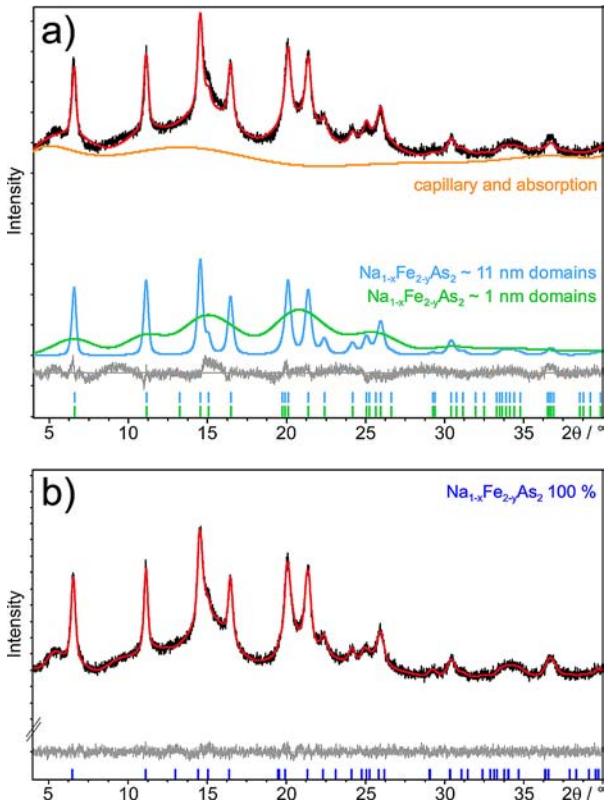

Figure 1. Observed (black) and calculated (red) powder X-ray diffraction pattern together with the difference profiles (gray) of the Rietveld refinements of $Na_{1-y}Fe_{2-x}As_2$. Peak positions are marked by vertical lines. (a) Fit resulting from the addition of a simple background function with 10 parameters (orange), 1 nm domains (green) and 11 nm domains (blue). (b) Fit with one phase and 36 parameters background function.

Table 1. Atomic Coordinates, Wyckoff Symbols, and Isotropic Displacement Parameters U_{iso} (Å^2) of $Na_{1-y}Fe_{2-x}As_2$, Space Group *I*4/*mmm*, *a* = 383.1(3) pm, *c* = 1252(2) pm, *Z* = 2[a]

atom	Wyckoff	*x*	*y*	*z*	U_{iso}	occ.
Na	2*a*	0	0	0	0.02(1)[b]	0.99(4)[c]
Fe	4*d*	0	1/2	1/4	0.020(6)	0.81(2)
As	4*e*	0	0	0.3662(5)	0.038(5)	1

[a] R_{wp} = 1.097, R_p = 0.881, χ^2 = 0.97, R_{Bragg} = 0.0985. [b] Restrained as maximum value. [c] Restrained to occ. ≤ 1.

Table 2 shows results of the EDX nanoprobe measurements. All areas reveal iron deficiency, the mean value is 1.7(1) in agreement with the Rietveld refinement of the PXRD data, and with the fact that dissolved iron ions were detected in the THF solution after the reaction. The sodium content fluctuates much stronger and results in a mean value of 0.9(2). Even though some areas are close to the 122-stoichiometry, the EDX-results clearly indicate fluctuating iron and also sodium concentrations. We assume that especially the sodium disorder is responsible

dx.doi.org/10.1021/ic3005618 | Inorg. Chem. 2012, 51, 8161−8167

Table 2. EDX Nanoprobe Analysis of $Na_{1-y}Fe_{2-x}As_2$[a]

no.	Na	Fe	As	Na/Fe/As
1	21.6	36.4	42.1	1.0: 1.7: 2
2	18.5	37.1	44.4	0.8: 1.7: 2
3	13.8	36.9	49.3	0.6: 1.5: 2
4	22.9	37.0	40.1	1.1: 1.9: 2
5	24.1	36.4	39.5	1.2: 1.8: 2
6	19.1	35.6	45.3	0.8: 1.6: 2
7	19.5	35.6	44.9	0.9: 1.6: 2
8	17.1	37.7	45.1	0.8: 1.7: 2
9	19.5	36.8	43.7	0.9: 1.7: 2
Ø				**0.9(2): 1.7(1): 2**

[a]Values are given in atom-% and also normalized to 1:2:2 stoichiometry assuming fully occupied arsenic.

for the low crystallinity and thus the broadening of the X-ray diffraction peaks.

Figure 2 shows the crystal structures of the precursor NaFeAs and the product $Na_{1-y}Fe_{2-x}As_2$. Both compounds

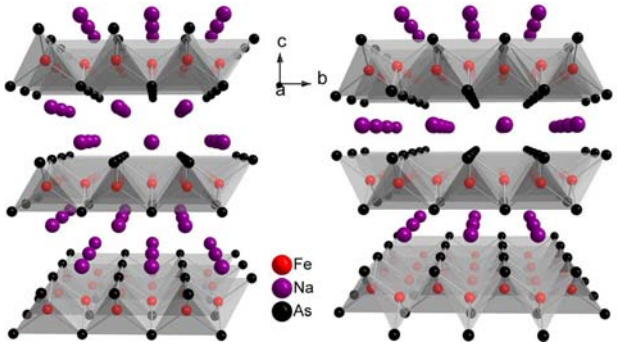

Figure 2. Crystal structures of NaFeAs (left) and $Na_{1-y}Fe_{2-x}As_2$ (right).

contain layers of edge-sharing $FeAs_{4/4}$ tetrahedra, which are separated either by double layers of sodium ions in NaFeAs or by single layers of sodium atoms in $Na_{1-y}Fe_{2-x}As_2$. Thus in the course of the topochemical transformation from NaFeAs to $Na_{1-y}Fe_{2-x}As_2$, half of the sodium ions are removed, and every second FeAs-layer has to slide 1/2 period along the lattice parameter *b* (Figure 2). The body-centered tetragonal structure (space group *I*4/*mmm*) of $Na_{1-y}Fe_{2-x}As_2$ is a minimal non-isomorphic *klassengleiche* supergroup of space group *P*4/*nmm* adopted by NaFeAs.

The Fe−As distance of 240.5(12) pm is typical for iron−arsenide superconductors, and also the slightly elongated $FeAs_4$ tetrahedron in terms of the 2-fold As−Fe−As angle (105.6(8)°) has been observed, for example, in KFe_2As_2 (107.02(5)°). Remarkably, the arsenic atoms of adjacent layers remain in a nonbonding state according to a distance of 335.0(9) pm in spite of the much smaller radius of Na^+ (116 pm) in comparison to K^+ (151 pm).

Magnetism and ^{57}Fe−Mössbauer spectroscopy. The magnetic susceptibilty of $Na_{1-y}Fe_{2-x}As_2$ was measured in a 15 Oe magnetic field under zero-field-cooled (zfc) and field-cooled (fc) conditions (Figure 3). Strong diamagnetism associated with the shielding-/Meissner-effect of superconductivity was detected below a critical temperature of 11 K. In contrast to this, Gooch et al.[13] reported a weak onset of diamagnetism already at 25 K prior to a steep decrease of the susceptibilty below 10 K. The 25 K feature is not visible in our

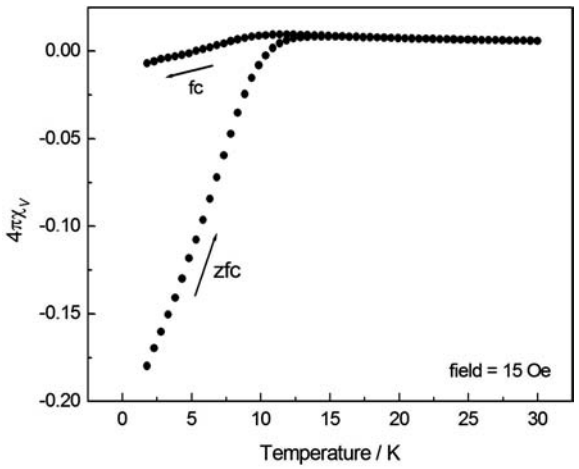

Figure 3. Magnetic susceptibility of $Na_{1-y}Fe_{2-x}As_2$.

measurement, while the second transition near to 11 K is observed in our sample. Todorov et al. likewise reported a critical temperature around 25 K, but for sodium-deficient $Na_{1-x}FeAs$ with 111-type structure, while a T_c of 12 K has been assigned to a compound referred to as $NaFe_2As_2$, which is in agreement with our results.[15] From this we suspect that the 25 K transition reported in ref 13 is due to a small impurity of sodium deficient $Na_{1-x}FeAs$.

The estimated superconducting volume fraction is about 20%, which can safely be assigned to $Na_{1-y}Fe_{2-x}As_2$ because no residual NaFeAs is discernible in the X-ray powder pattern. However, the relatively broad transition indicates a certain distribution of the composition. One may assume that the superconducting phase is close to or even identical with the stoichiometric (1:2:2), however, from our data it is only clear that the superconducting phase has the 122-type structure, while the exact composition with respect to the values of *x* and *y* in the superconducting fraction of $Na_{1-y}Fe_{2-x}As_2$ is still an open question.

Figure 4 presents ^{57}Fe Mössbauer spectra of the $Na_{1-y}Fe_{2-x}As_2$ sample at 298, 80, and 4.2 K together with transmission integral fits. The corresponding fitting parameters are listed in Tab. 3. All three spectra are well reproduced with single signals which were subjected to weak quadrupole splitting. The increase of the isomer shift with decreasing temperature (0.24 → 0.38 mm/s) is a consequence of a second order Doppler shift, similar to our recent investigations on $SrFe_2As_2$, SrFeAsF, and KFe_2As_2.[16−18] Weak quadrupole splitting results from a deviation from ideal tetrahedral $FeAs_{4/4}$ coordination.

In contrast to other iron arsenides, we observe a significant increase of the experimental line width. Although one might expect that the small refined quadrupole splitting parameters and the increased line width parameters might correlate, the high quality of the fits clearly point to the increased line width parameters. We ascribe this line width increase to the distribution of very small sized domains within the $Na_{1-y}Fe_{2-x}As_2$ particles. Such a behavior has also been observed for amorphous SnO_2,[19] which shows much higher line width than well crystallized SnO_2. Another reason might be the homogeneity range of $Na_{1-y}Fe_{2-x}As_2$. ^{57}Fe Mössbauer spectra of NaFeAs reported by Todorov[15] showed higher isomer shifts than the $Na_{1-y}Fe_{2-x}As_2$ sample reported herein. Since we observe no shoulder in our spectra at higher velocity, we can

dx.doi.org/10.1021/ic3005618 | Inorg. Chem. 2012, 51, 8161−8167

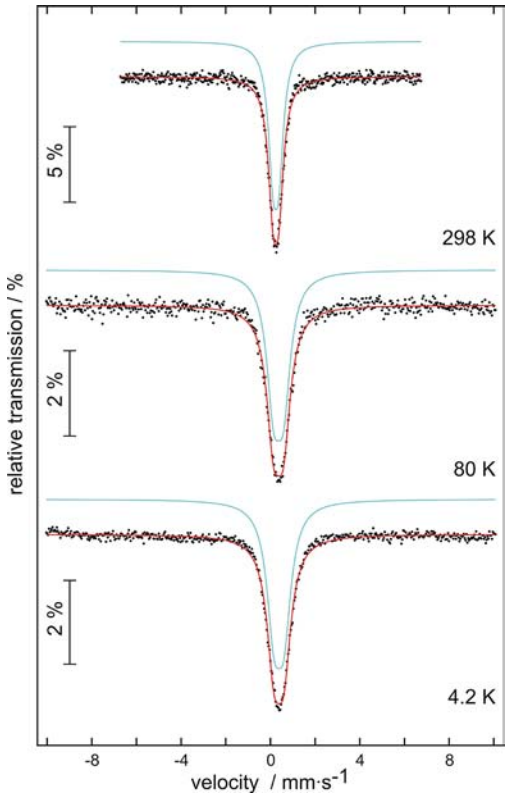

Figure 4. Experimental and simulated ^{57}Fe Mössbauer spectra of $Na_{1-y}Fe_{2-x}As_2$ at 298, 80, and 4.2 K.

Table 3. Fitting Parameters of the ^{57}Fe Mössbauer Spectra of $Na_{1-y}Fe_{2-x}As_2$ at Different Temperatures[a]

T (K)	δ (mm·s^{-1})	Γ (mm·s^{-1})	ΔE_Q (mm·s^{-1})
298	0.24(1)	0.52(1)	0.26(1)
80	0.36(1)	0.77(2)	0.44(1)
4.2	0.38(1)	0.78(1)	0.44(1)

[a]Numbers in parentheses represent the statistical errors in the last digit. (δ) isomer shift; (Γ) experimental line width, (ΔE_Q) quadrupole splitting parameter.

exclude a notable residual NaFeAs in our sample in agreement with the PXRD and TEM. No magnetic hyperfine field splitting is evident down to 4.2 K. This is another hint for the purity of our sample, since NaFeAs shows charge-density-wave formation below 40 K with a small, but notable hyperfine field at low temperatures.

Solid-State NMR Spectroscopy. So far all results consistently point to deviations from the ideal 1:2:2 composition in $Na_{1-y}Fe_{2-x}As_2$. In order to examine this finding more closely, we have further analyzed the sample by ^{23}Na solid-state NMR spectroscopy and transmission electron microscopy (TEM).

^{23}Na MAS spectra of $Na_{1-y}Fe_{2-x}As_2$ have been measured, and for comparison also of the precursor NaFeAs and $Ba_{0.6}Na_{0.4}Fe_2As_2$, the latter has an inherent Ba/Na site disorder (Figure 5). Moreover we obtained T_1 relaxation time constants in order to get an indication whether relaxation contributes differently to the line width via lifetime broadening of the resonances. However T_1 relaxation time constants at room temperature are all in the range of 0.3 ± 0.2s. We can also exclude a dominant contribution to the line width by the paramagnetic chemical shift caused by hyperfine coupling to unpaired electron spins because the observed chemical shift values hardly change when the sample temperature is increased by about 10 K. Furthermore we have estimated the quadrupole coupling constant C_Q of NaFeAs at room temperature from a ^{23}Na satellite transition MAS NMR spectrum[20] ($|C_Q|$ = 0.9 MHz, not shown) and that of $NaFe_2As_2$ theoretically by DFT calculations (C_Q = 1.0 MHz). The asymmetry parameter, η_Q is zero by symmetry in both cases. The expected second-order quadrupolar broadening of the central transition is only of the order of 250 Hz under the chosen experimental conditions and thus not significant. The ^{23}Na line width of NaFeAs and of $Ba_{0.6}Na_{0.4}Fe_2As_2$ is an order of magnitude less than that of the title compound $Na_{1-y}Fe_{2-x}As_2$. We can exclude also second order quadrupolar shift, relaxation effects and a paramagnetic broadening mechanism as the source of broadening as shown above. Hence we conclude that the broadening of the ^{23}Na resonance gives evidence of disorder of Na on an atomic scale.

Transmission Electron Microscopy. According to bright field images, the sample does not contain nanoparticles but crystals with a low expansion of the coherently scattering domains/areas. This is consistent with the powder XRD pattern and explains the observed reflection profiles. EDX nanoprobe measurements indicate the absence of oxygen contaminations.

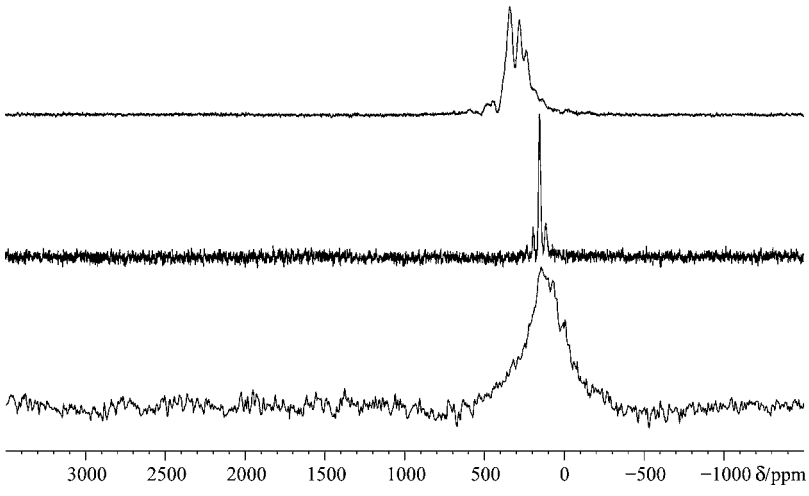

Figure 5. ^{23}Na solid-state MAS NMR spectra of $Na_{1-y}Fe_{2-x}As_2$ (bottom), NaFeAs (middle), and $Ba_{0.6}Na_{0.4}Fe_2As_2$ (top).

dx.doi.org/10.1021/ic3005618 | Inorg. Chem. 2012, 51, 8161−8167

Several crystals which can be assigned via electron diffraction to the $Na_{1-y}Fe_{2-x}As_2$-type structure were chemically analyzed by EDX (see Table 2). During the experiments it emerged that the crystallites are quite radiation sensitive under standard emission settings. However, when adjusting low-dose settings, particularly by reducing emission, the samples do not change significantly their structure and chemical composition within the time slice of observation. Remarkably, all crystals exhibit planar defects which are well seen even immediately after the initial irradiation. Thus, the defects represent an intrinsic real structural feature and no artifact produced by electron beam impact. When adjusting the crystals along the zone axis [100], cf. Figure 6a, the planar defects appear as stripes parallel to the

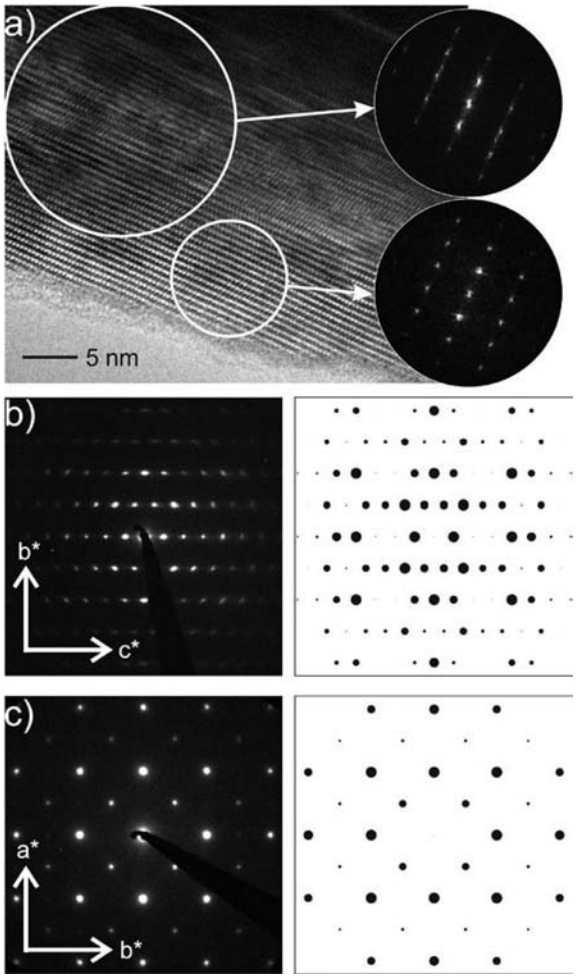

Figure 6. (a) HRTEM micrograph recorded on $Na_{1-y}Fe_{2-x}As_2$, zone axis [100] with attached Fourier transforms from the highlighted circular areas. (b and c) PED patterns (each left) and simulated patterns (each right) for the zone axes [100] and [001], respectively.

planes (001) in high resolution contrast. The presence of (001) defects is further supported by the presence of diffuse 00*l*-streaks in Fourier transforms of HRTEM micrographs (see Fourier transform from larger circle attached to Figure 6a). However in smaller areas the structure and the corresponding Fourier transforms do not exhibit any indication for disordering, cf. Fourier transform from the smaller circle attached to Figure 6a. Generally the PEDs which are recorded on large circular areas (diameter 250 nm) clearly show the diffuse streaks. Note, that all Bragg intensities are streaked, thus, the sizes of the perfectly crystalline areas are small. The PED patterns (e.g., Figure 6b, 6c, each left) recorded on single crystalline areas comply with the structure model from powder XRD as indicated by the convincing agreement with simulated patterns based on the kinematic approximation (Figure 6b, 6c, each right).

The local view on the structure by high-resolution imaging is demonstrated by the micrograph of Figure 7. The image was

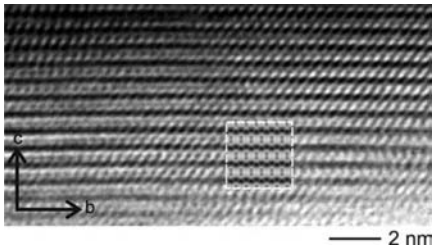

Figure 7. High resolution micrograph after Fourier filtering and inserted simulation for zone axis [100]. Parameters for simulation: thickness 3.8 nm, $\Delta f = -65$ nm.

recorded close to Scherzer focus, thus, the dark contrasts correlate with the positions of the heavy atoms Fe and As, as indicated by the inserted simulated micrograph. The layered arrangement of these atoms along [010] is clearly seen, but the correlation between experimental and simulated micrograph is not perfect. However, such deviations are expected since the structure model for the simulation is based on the PXRD results, which take not into account local deformations of the structure by fluctuations of the chemical composition, particularly concerning the Na content.

CONCLUSION

We have presented a reproducible synthesis method and an extensive characterization of the iron arsenide $Na_{1-y}Fe_{2-x}As_2$. Our results show that the metastable compound has a deficient $ThCr_2Si_2$-type structure with mean compositions $Na_{0.9(2)}Fe_{1.7(2)}As_2$ from EDX and $Na_{0.99(4)}Fe_{1.67(2)}As_2$ from Rietveld-refinements. Electron microscopy detects well crystalline and strongly distorted areas associated with a significant disorder of sodium in agreement with ^{23}Na-NMR data. This is probably the origin of the poor crystallinity of the sample that reduces the accuracy of the X-ray powder diffraction experiment. However we could show that the large scattering background is caused by very small domain sizes of $Na_{1-y}Fe_{2-x}As_2$, and not by an amorphous foreign phase. This is supported by the ^{57}Fe Mössbauer spectrum which shows only one type of iron on the local scale. From this we infer that the sample is one crystallographic phase which suffers from fluctuating composition and very small coherently scattering domains. The latter is probably a consequence of the heterogeneous solid/liquid reaction at low temperature. We note that the exact composition of the compounds referred to as $NaFe_2As_2$ in two earlier reports[13,15] has not been scrutinized. Our ac-susceptibility measurements reveal one superconducting transition at 11 K in agreement with the main transition in ref.,[13] and also with the transition that has been associated to $NaFe_2As_2$ in ref 15. However, the shielding fraction is only 20% and with respect to the observed fluctuations of sodium and iron occupations, the true composition of the superconducting phase remains still unclear. Anyway the critical temperature of $Na_{1-y}Fe_{2-x}As_2$ is about three times higher than those of the

dx.doi.org/10.1021/ic3005618 | Inorg. Chem. 2012, 51, 8161−8167

higher homologues (K, 3.8 K; Rb and Cs, 2.6 K), and one may argue if this is a volume effect or connected to the nonstoichiometry. The iron deficiency is actually surprising because electron counting according to $Na^{+}_{\sim 1}Fe^{3+}_{1.67}As_2$ reveals Fe^{3+}, equivalent to very strong hole doping. This would mean that T_c increases again beyond the hole-overdoped stoichiometric compounds $(K,Rb,Cs)Fe_2^{2.5+}As_2$, which is appealing, but rather unlikely. We rather suggest that superconductivity occurs in the more ordered fractions of the sample indicated in the HRTEM mappings, where the chemical composition is near to, or even exactly $NaFe_2As_2$.

Even though the crystallinity of the compound is still rather poor, we point out that this material represents the first metastable iron-based superconductor. This can pave the way to new iron-based superconducting materials, which are not accessible by high temperature methods.

EXPERIMENTAL SECTION

NaFeAs. The NaFeAs precursor was synthesized through solid state reaction from Na (99.8%) and FeAs, sealed in a welded niobium crucible and placed into a fused silica ampule under argon. The mixture was heated to 973 K for 48 h at 50 K/h and then cooled to room temperature at 150 K/h. Powder X-ray diffraction showed single phase NaFeAs.

$Na_{1-y}Fe_{2-x}As_2$. To obtain $Na_{1-y}Fe_{2-x}As_2$ from NaFeAs (0.40 g, 2.60 mmol) the precursor was oxidized with iodine (0.53 g, 2.08 mmol, 0.8 equiv). The reagents were separately dispersed (NaFeAs) and solved (I_2) in THF (30−36 mL) respectively, whereby Schlenk's technique with purified Argon as inert gas was used for the whole experiment. The polar-aprotic solvent THF was dried over sodium and benzophenone and was freshly distilled prior to use. The iodine solution was added slowly to NaFeAs (approximately 40 min.). The reaction mixture was stirred for 40 h at room temperature, than the solid product $Na_{1-y}Fe_{2-x}As_2$, which is gray with metallic luster, was filtered off and was dried under high vacuum.

X-ray Powder Diffraction. X-ray powder diffraction patterns were recorded on a STOE Stadi P ($Mo_K\alpha_1$ radiation, Ge (111) primary monochromator, λ = 70.93 pm, silicon as external standard, rotating capillary 0.2 mm outer diameter). Rietveld refinements were performed with the TOPAS program package.[21] To generate the reflection profiles the fundamental parameters approach was used. The preferred orientation of the crystallites was described with fourth-order spherical harmonics.

Magnetic Measurements. A commercial Quantum Design MPMS XL5 SQUID magnetometer was used at temperatures between of 1.8 and 300 K. The polycrystalline sample was ground and filled into a gelatin capsule, which was fixed in a plastic straw. The magnetic measurements were performed with the MPMS MultiVu software.

Mössbauer Spectroscopy. For the ^{57}Fe−Mössbauer spectra a ^{57}Co/Rh source was used. The sample was placed in thin-walled PVC containers at thicknesses of about 4−10 mg Fe/cm^2. The measurements were performed in transmission geometry at different temperatures. Fitting of the spectra was carried out with the NORMOS-90 program package.[22]

Solid-State NMR. NMR experiments were performed on a Bruker AVANCEIII spectrometer equipped with an 11.7 T magnet and commercial magic-angle spinning probes. The samples were diluted with BaF2 to allow sample spinning frequencies between 2 and 25 kHz in ZrO_2 rotors. The experimental conditions were chosen so that the spectra reflect the ^{23}Na central transitions only. T_1 relaxation time constants were obtained with the saturation recovery experiment. The chemical shift scale refers to 0.1 mol/L NaCl in D_2O at 0 ppm.

High Resolution Transmission Electron Microscopy. SAED (selected area electron diffraction) and PED (precession electron diffraction, precession angle = 3°) were performed with a Philips CM30 ST microscope (300 kV, LaB6 cathode, C_S = 1.15 mm). All manipulations for the preparation and transfer of the sample were carried out under Ar with the aid of a self-constructed device.[23,24] Simulations of HRTEM images (multislice formalism) were calculated with the EMS program package[25] (spread of defocus = 70 Å, illumination semiangle = 1.2 mrad). All images were evaluated (including Fourier filtering) with the program Digital Micrograph 3.6.1 (Gatan). HRTEM images were filtered after Fourier transformation (ABSF). Elemental analyses by EDX were performed in the nanoprobe mode with a Si/Li detector (Noran NSF 7).

AUTHOR INFORMATION

Corresponding Author

*E-mail: johrendt@lmu.de. Phone: +49 (0)89 218077430. Fax: +49 (0)89 218077431.

Notes

The authors declare no competing financial interest.

ACKNOWLEDGMENTS

We thank Christian Minke for help with the NMR experiments, Franziska Hummel for performing DFT calculations and Dr. Marcus Tegel for help with Rietveld refinements. This work was financially supported by the European Commission within the SUPER-IRON project and by the German Research Foundation (DFG) within SPP 1458.

REFERENCES

(1) Johrendt, D.; Pöttgen, R. *Angew. Chem., Int. Ed.* **2008**, *47*, 4782−4784.
(2) Johnston, D. C. *Adv. Phys.* **2010**, *59*, 803−1061.
(3) Kamihara, Y.; Watanabe, T.; Hirano, M.; Hosono, H. *J. Am. Chem. Soc.* **2008**, *130*, 3296−3297.
(4) Rotter, M.; Tegel, M.; Johrendt, D. *Phys. Rev. Lett.* **2008**, *101*, 107006.
(5) Parker, D. R.; Pitcher, M. J.; Baker, P. J.; Franke, I.; Lancaster, T.; Blundell, S. J.; Clarke, S. J. *Chem. Commun.* **2009**, 2189−2191.
(6) Johrendt, D.; Hosono, H.; Hoffmann, R.-D.; Pöttgen, R. *Z. Kristallogr.* **2011**, *226*, 435−446.
(7) de la Cruz, C.; Huang, Q.; Lynn, J. W.; Li, J. Y.; Ratcliff, W.; Zarestky, J. L.; Mook, H. A.; Chen, G. F.; Luo, J. L.; Wang, N. L.; Dai, P. C. *Nature* **2008**, *453*, 899−902.
(8) Zinth, V.; Dellmann, T.; Klauss, H.-H.; Johrendt, D. *Angew. Chem., Int. Ed.* **2011**, *50*, 7919−7923.
(9) Johrendt, D. *J. Mater. Chem.* **2011**, *21*, 13726−13736.
(10) Ren, Z.-A.; Lu, W.; Yang, J.; Yi, W.; Shen, X.-L.; Li, Z.-C.; Che, G.-C.; Dong, X.-L.; Sun, L.-L.; Zhou, F.; Zhao, Z.-X. *Chin. Phys. Lett.* **2008**, *25*, 2215.
(11) Hiramatsu, H.; Katase, T.; Kamiya, T.; Hirano, M.; Hosono, H. *Appl. Phys. Lett.* **2008**, *93*, 162504.
(12) Hiramatsu, H.; Katase, T.; Kamiya, T.; Hirano, M.; Hosono, H. *Appl. Phys. Express* **2008**, *1*, 101702.
(13) Gooch, M.; Lv, B.; Sasmal, K.; Tapp, J. H.; Tang, Z. J.; Guloy, A. M.; Lorenz, B.; Chu, C. W. *Phys. C: Superconductivity* **2010**, *470*, S276.
(14) Sasmal, K.; Lv, B.; Tang, Z. J.; Chen, F.; Xue, Y. Y.; Lorenz, B.; Guloy, A. M.; Chu, C. W. *Phys. Rev. B* **2009**, *79*, 184516.
(15) Todorov, I.; Chung, D. Y.; Claus, H.; Malliakas, C. D.; Douvalis, A. P.; Bakas, T.; He, J.; Dravid, V. P.; Kanatzidis, M. G. *Chem. Mater.* **2010**, *22*, 3916−3925.
(16) Tegel, M.; Rotter, M.; Weiss, V.; Schappacher, F.; Pöttgen, R.; Johrendt, D. *J. Phys.: Condens. Matter* **2008**, *20*, 452201.
(17) Tegel, M.; Johansson, S.; Weiss, V.; Schellenberg, I.; Hermes, W.; Pöttgen, R.; Johrendt, D. *Europhys. Lett.* **2008**, *84*, 67007−67011.
(18) Rotter, M.; Tegel, M.; Schellenberg, I.; Schappacher, F. M.; Pöttgen, R.; Deisenhofer, J.; Gunther, A.; Schrettle, F.; Loidl, A.; Johrendt, D. *New J. Phys.* **2009**, *11*, 025014.
(19) Collins, G. S.; Kachnowski, T.; Benczer-Koller, N.; Pasternak, M. *Phys. Rev. B* **1979**, *19*, 1369−1373.
(20) Jakobsen, H. J.; Skibsted, J.; Bildsøe, H.; Nielsen, N. C. *J. Magn. Reson.* **1989**, *85*, 173.

(21) Coelho, A. *TOPAS-Academic*, version 4.1; Coelho Software: Brisbane, Australia, 2007.
(22) Brand, R. A. *Normos Mössbauer Fitting Program*; Universität Duisburg: Essen, Germany; 2002.
(23) Jeitschko, P.; Simon, A.; Ramlau, R.; Mattausch, H. *Z. Anorg. Allg. Chem.* **1997**, *623*, 1447.
(24) Jeitschko, P.; Simon, A.; Ramlau, R.; Mattausch, H. *Eur. Microsc. Microanal.* **1997**, *46*, 21.
(25) Stadelmann, A. *Ultramicroscopy* **1987**, *21*, 131.